



## Growth and Characterization of Non-Linear Optical Single Crystal Guanidinium triscadmium Sulphate Octahydrate

A. RAJESWARI<sup>1,2</sup> and P. MURUGAKOOTHAN<sup>1,\*</sup>

<sup>1</sup>MRDL, PG and Research Department of Physics, Pachaiyappa's College, Chennai-600030, India

<sup>2</sup>Department of Physics, S.D.N.B. Vaishnav College for Women, Chennai-600044, India

\*Corresponding author: E-mail: murugakoothan03@yahoo.co.in

Received: 24 September 2018;

Accepted: 30 November 2018;

Published online: 31 January 2019;

AJC-19265

Semi-organic single crystals of guanidinium tris cadmium sulphate octahydrate (GuCdS) with nonlinear optical properties were successfully grown by slow solvent evaporation technique. The grown crystals were characterised by powder X-ray diffraction analysis to determine the unit cell parameters. The structure of the compound belongs to triclinic crystal system and space group is found to be  $P\bar{1}$ . The grown crystals were subjected to FTIR spectroscopic analysis to confirm the presence of functional groups present in the compound. UV-vis-NIR spectral study suggested that the grown crystal is transparent in the entire visible region, the lower cut off wavelength is 200 nm and the band gap value is estimated to be 6.14 eV. Nonlinear refractive index ( $n_2$ ), absorption coefficient ( $\beta$ ) and third order nonlinear susceptibility ( $\chi^{(3)}$ ) were calculated using Z-scan technique. The thermal stability of grown crystal was investigated by thermogravimetric and differential thermogravimetric analyses. The dielectric behaviour of the grown crystal was analyzed as a function of frequency of the applied field. The mechanical properties of grown crystal were examined by Vickers's micro hardness test. The laser damage threshold of the grown crystal was calculated to be 1.796 GW/cm<sup>2</sup>.

**Keywords:** Nonlinear Optical Material, Guanidinium tris cadmium sulphate octahydrate, Band gap, Thermal properties.

### INTRODUCTION

The growth of single crystals and their characterisation towards device fabrication have gained more interest due to their significant applications in the fields of semiconductors, solid state lasers, nonlinear optics, piezoelectric, photosensitive materials and crystalline thin films for microelectronics and computer industries. In particular the non linear optics plays a major role in the emerging areas of laser technology, optical communication, data storage technology, photonics and optoelectronics. Hence, nonlinear optical materials are important for future photonic technologies as well as the growth of promising new nonlinear optical materials receive great attention [1].

Many organic and inorganic nonlinear optical materials have been reported in the literature with good optical, thermal and mechanical properties. In comparison with these crystals, the semi organic nonlinear optical crystal possesses the advantage of both organic as well as inorganic materials. They have

high damage threshold, wide transparency range, excellent nonlinear optical coefficient and superior mechanical properties [2,3].

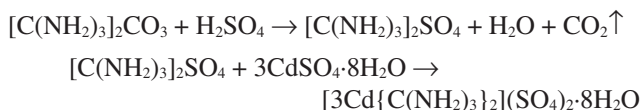
Guanidinium based organic and inorganic compounds play a vital role in the field of nonlinear optical crystal growth. The guanidinium ion  $[C(NH_2)_3]^+$  is an important functional group present in the amino acid and also the basic component of many biologically active molecule [4]. Different derivatives of guanidinium ion are used in explosives and rocket repellent formulations [5]. It is a strong base which reacts with most of the organic acid resulting in the formation of guanidinium species. The three-fold symmetry of guanidinium ion with six equivalent hydrogen atoms provides excellent condition for hydrogen bonding and this property has made guanidinium compounds as prospective materials in the field of nonlinear optical crystal growth and their applications.

The crystal structure, vibrational spectroscopic studies and ferroelectric properties of some guanidinium metal sulphates have been reported in the literature [6-8]. Many guanidinium

based nonlinear optical crystals were grown and reported [9,10]. In this paper, we delineate the growth and characterisation studies of guanidinium *tris* cadmium sulphate octahydrate (GuCdS).

## EXPERIMENTAL

**Synthesis and crystal growth:** Guanidinium cadmium sulphate octahydrate compounds were synthesized using AR grade reagents guanidinium carbonate, conc. sulphuric acid and cadmium sulphate octahydrate taken in an equimolar stoichiometric ratio. Distilled water was used as solvent and the crystallization was carried out at room temperature. The solution was stirred well using magnetic stirrer for 6 h to ensure the homogenous concentration and it was filtered using Whatmann filter paper and kept for slow evaporation of solvent in a dust free atmosphere. The pH value of solution was found to be at 1. After a few days, guanidinium *tris* cadmium sulphate octahydrate (GuCdS) compound was found to crystallize at the bottom of beaker. The following equation represents the scheme of synthesis.



The synthesised compound was purified further by repeated recrystallization with the same solvent and used for the growth of the bulk crystal. A saturated aqueous GuCdS solution was prepared from the recrystallized salt guanidinium cadmium sulphate and allowed to evaporate in a dust free atmosphere. After 13 days transparent, defect free single crystals of guanidinium cadmium sulphate were harvested (Fig. 1).

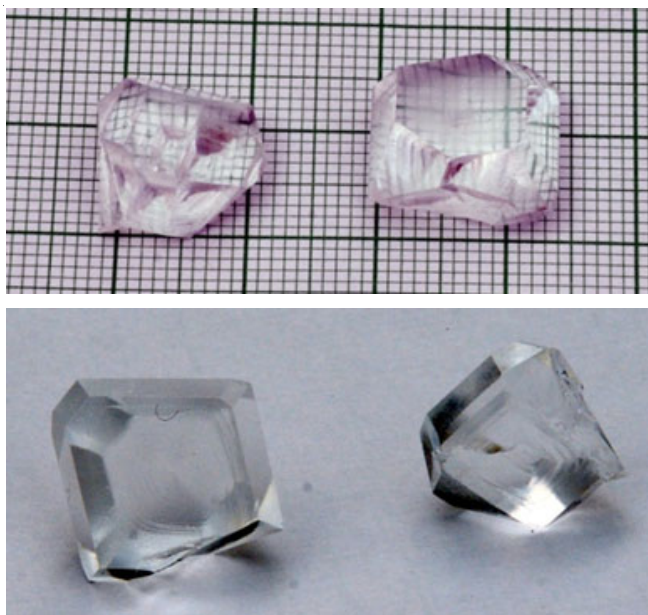


Fig. 1. As grown GuCdS crystal

## RESULTS AND DISCUSSION

**Powder X-ray diffraction analysis:** The powder pattern of a crystal is very important in determining the crystallinity and phase purity of the grown crystal. The powder X-ray diffraction analysis of the grown crystal was recorded using RICH SIEFERT powder X-ray diffractometer with  $\text{CuK}\alpha$  ( $\lambda = 1.5406 \text{ \AA}$ ) radiation. Grown crystals were ground using agate mortar and pestle and put through to powder X-ray diffraction analysis. The sample was scanned in the range  $10^\circ$ - $70^\circ$  in steps of  $0.04^\circ$ . The powder X-ray diffraction spectrum of the grown crystal is shown in Fig. 2. The intense and sharp peaks in the diffractogram indicate the good crystalline perfection of the grown crystals. The  $2\theta$  values obtained from the powder X-ray analyses were used for indexing the powder pattern. The indexing of peaks and the estimation of lattice cell parameters were carried off using the powder X software. It was found that the grown crystal GuCdS falls under triclinic crystal system and the space group was found to be  $P\bar{1}$ , which is a centrosymmetric crystal. The obtained cell parameters of the crystal are  $a = 6.444 \text{ \AA}$ ,  $b = 6.456 \text{ \AA}$ ,  $c = 10.020 \text{ \AA}$ ,  $\alpha = 90.16^\circ$ ,  $\beta = 97.035^\circ$  and  $\gamma = 110^\circ$ . The calculated lattice cell parameter values agreed well with the reported values and presented in Table-1.

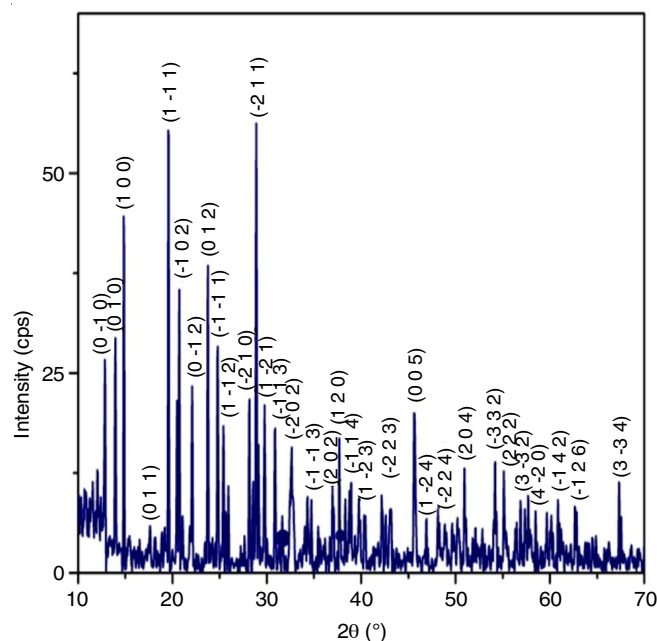


Fig. 2. Powder X-ray diffraction pattern of GuCdS crystalline sample

**FTIR analysis:** The FTIR spectrum of powdered sample was recorded using Perkin Elmer Spectrum-1 in the range  $4000$  to  $450 \text{ cm}^{-1}$ . The allotment of spectral bands were carried out in terms of fundamental modes of vibration of guanidinium ion  $[\text{C}(\text{NH}_2)_3]^+$ , sulphate ion  $(\text{SO}_4^{2-})$  and water molecules [7]. The recorded FTIR spectrum of guanidinium cadmium sulphate is shown in Fig. 3.

TABLE-1  
CELL PARAMETERS OF GuCdS

GuCdS	a (Å)	b (Å)	c (Å)	$\alpha$ (°)	$\beta$ (°)	$\gamma$ (°)	V (Å <sup>3</sup> )
Reported [Ref. 6]	6.441	6.459	10.015	90.18	97.02	110.00	386.3
Present study	6.444	6.456	10.020	90.16	97.03	109.97	388.4

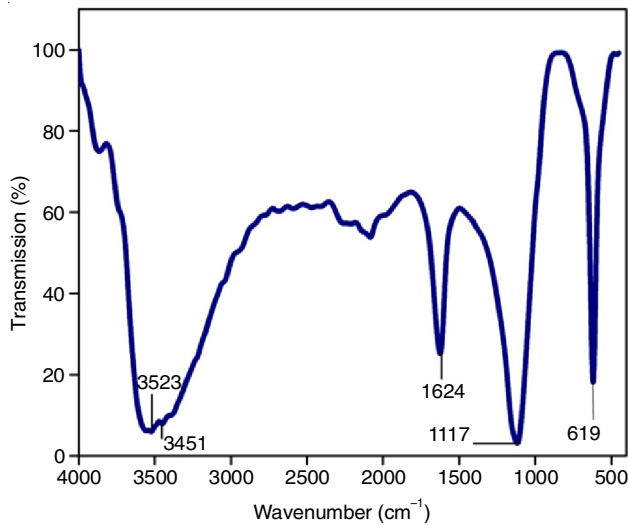


Fig. 3. FTIR spectrum of GuCdS crystalline sample

**Vibrations of guanidinium ions:** The assignment of vibrational modes in guanidinium ion can be done in terms of  $\text{CN}_3$  and  $\text{NH}_2$  groups. In IR spectrum of GuCdS compound, a sharp strong band at  $1624 \text{ cm}^{-1}$  is due to asymmetric stretching vibrations of  $\text{CN}_3$  group.

**Vibrations of sulphate group:** The sulphate group in its free ion state exhibit four fundamental modes of vibration. The modes are non-degenerate symmetric stretching mode ( $\nu_1$ ), doubly degenerate symmetric bending mode ( $\nu_2$ ), triply degenerate asymmetric stretching mode ( $\nu_3$ ) and the triply degenerate asymmetric bending mode ( $\nu_4$ ) with wave numbers  $981, 451, 1108$  and  $613 \text{ cm}^{-1}$ , respectively. Among the four different modes of vibration only ( $\nu_3$ ) and ( $\nu_4$ ) are IR active. The triply degenerate asymmetric stretching ( $\nu_3$ ) mode of sulphate ion has a strong band at  $1117 \text{ cm}^{-1}$  and the triply degenerate asymmetric bending mode ( $\nu_4$ ) appears at  $619 \text{ cm}^{-1}$  in the FTIR spectrum.

**Vibrations of water molecule:** A water molecule in general has three fundamental modes of vibration: ( $\nu_1$ ) at  $3652 \text{ cm}^{-1}$ , ( $\nu_2$ ) at  $1595 \text{ cm}^{-1}$  and ( $\nu_3$ ) at  $3756 \text{ cm}^{-1}$ . The IR spectrum of GuCdS compound contains strong bands at  $3451$  and  $3523 \text{ cm}^{-1}$  which are assigned to  $\nu_1$  and  $\nu_3$  vibrational modes of water molecule. The vibrational band assignments of FTIR spectrum of grown crystal was found to be consistent with that of the values reported in the literature [11]. The experimental vibrational frequencies of GuCdS are presented in Table-2.

TABLE-2  
VIBRATIONAL BAND ASSIGNMENTS OF GuCdS

Wavenumber ( $\text{cm}^{-1}$ )	Band assignment
619 m	$\nu_4(\text{SO}_4)$
1117 s	$\nu_3(\text{SO}_4)$
1624 m	$\nu_{\text{as}}(\text{CN}_3)$
3451 s	$\nu_1(\text{H}_2\text{O})$
3523 s	$\nu_3(\text{H}_2\text{O})$

m = medium; s = strong;  $\nu_{\text{as}}$  = asymmetric stretching

**UV-vis-NIR analysis:** UV-vis-NIR spectral study was performed for the grown crystal in the range between 200-1100 nm by Perkin-Elmer UV spectrophotometer. The optical transmission range and transparency cut off are the most

important optical parameters for laser frequency conversion applications [12]. For optical device fabrication the crystal should have good transmission in a wide scale of wavelength. From the transmission spectrum, it is clear that the as grown GuCdS crystal is optically transparent in the ultraviolet, entire visible and near infra red region (Fig. 4). The transparency is about 80 % in the entire visible and IR regions and the lower cut off wavelength is found to be at 200 nm.

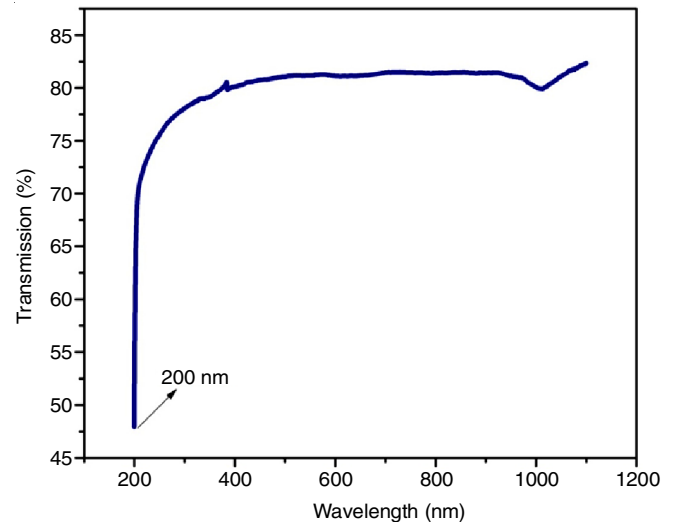


Fig. 4. UV-vis-NIR transmission spectrum of GuCdS crystal

This transmission window (200-1100 nm) is suitable for the generation of second harmonics ( $\lambda = 532 \text{ nm}$ ) as well as third harmonics ( $\lambda = 354 \text{ nm}$ ) of Nd:YAG laser of wavelength  $1064 \text{ nm}$  [13].

**Determination of optical constants:** The values of optical constants such as optical band gap, extinction coefficient and refractive index are important in order to analyze the potential applications of the grown crystal in the field of optoelectronics. The transmission data was used to determine the optical constants such as absorption coefficient ( $\alpha$ ), extinction coefficient ( $k$ ) and the refractive index ( $n$ ) of the grown GuCdS crystal.

The optical absorption coefficient ( $\alpha$ ) was determined from the transmission data using the following expression reported in the literature [14]:

$$\alpha = \frac{2.303 \log\left(\frac{1}{T}\right)}{t} \quad (1)$$

In the above equation, T represents the transmittance value and t is the thickness of the crystal. The optical band gap energy was calculated from the transmission spectrum using the following expression [14]:

$$(\alpha h\nu)^2 = A(E_g - h\nu) \quad (2)$$

where h is the Planck's constant,  $E_g$  is the optical band gap energy of the crystal,  $\alpha$  is the optical absorption coefficients near the absorption edge and A is a constant. The Tauc's plot was drawn between photon energy ( $h\nu$ ) and  $(\alpha h\nu)^2$  and from the plot the band gap of crystal was estimated by the extrapolation of linear portion of the graph to photon energy axis.

The value is found to be 6.14 eV as shown in Fig. 5. The value indicates that the GuCdS crystal is a high band gap energy material and can be suitable for UV tuneable laser.

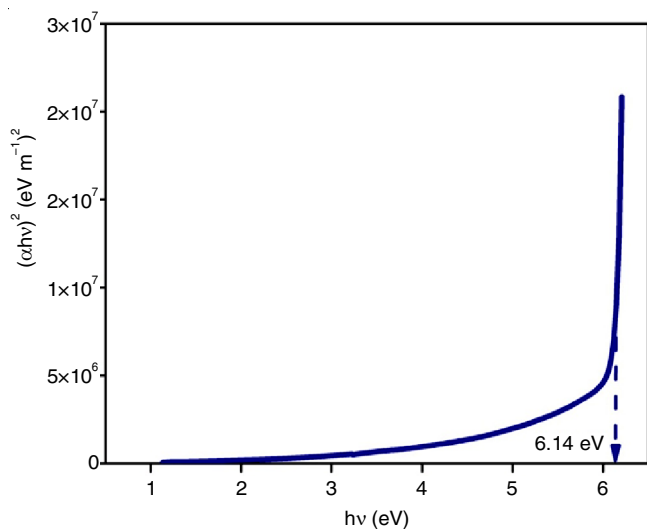


Fig. 5. Tauc's plot of GuCdS

The optical constants such as extinction coefficient ( $k$ ) and the refractive index ( $n$ ) were computed for GuCdS crystal using the expressions reported in the literature [15]. The reflectance ( $R$ ) values of grown crystal was calculated in terms of optical absorption coefficient ( $\alpha$ ) using the following expression [15]:

$$R = \frac{1 \pm \sqrt{1 - e^{(-\alpha t)} + e^{(\alpha t)}}}{1 + e^{(-\alpha t)}} \quad (3)$$

The refractive index ( $n$ ) of grown crystal was calculated using the values of reflectance ( $R$ ) by the following relation:

$$n = \frac{-(R+1) \pm \sqrt{3R^2 + 10R - 3}}{2(R-1)} \quad (4)$$

The extinction coefficient ( $k$ ) is the fraction of electromagnetic energy lost due to scattering and absorption per unit thickness in a particular medium which can be evaluated by the following expression:

$$k = \frac{\alpha \lambda}{4\pi} \quad (5)$$

The variation of refractive index ( $n$ ) and extinction coefficient ( $k$ ) values with wavelength are shown in Fig. 6. From this spectra, it is evident that values of refractive index ( $n$ ) and extinction coefficient ( $k$ ) strongly depend on the wavelength, particularly in the UV region. It is clear from the graph that the extinction coefficient increases for the increase in wavelength. The values of refractive index increase sharply in the UV region due to the absorption of photon by the crystal and the values remain almost constant in the visible region and IR region.

The optical conductivity ( $\sigma$ ) is a measure of the frequency response of material when irradiated with light and was calculated using the optical absorption coefficient ( $\alpha$ ) using the following relation [16]:

$$\sigma = \frac{\alpha n c}{4\pi} \quad (6)$$

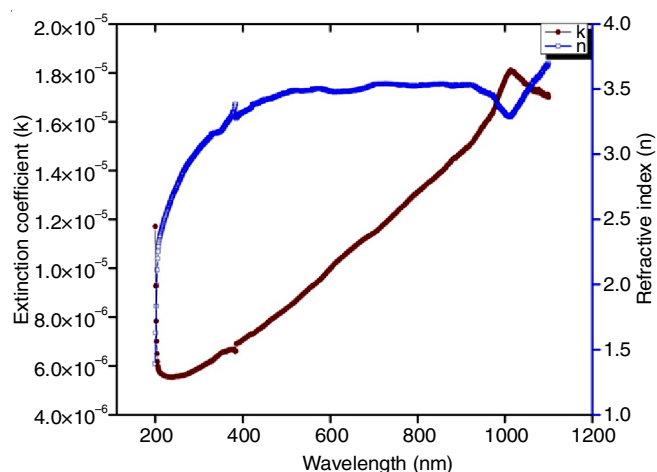


Fig. 6. Plot of wavelength vs. extinction coefficient and refractive index of GuCdS crystal

The calculated optical conductivity values are plotted against photon energy (Fig. 7). The graph represents that values of optical conductivity increases with increase of photon energy.

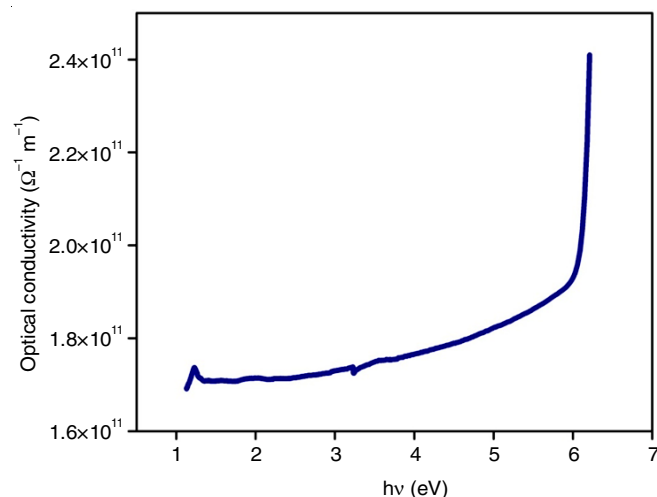


Fig. 7. Plot of photon energy vs optical conductivity

The optical studies disclosed that the GuCdS crystal possesses good optical characteristics and can be applied for optical device applications.

### Non-linear optical measurements

**Second harmonic generation (SHG) measurement:** The second harmonic generation efficiency of the grown GuCdS crystal was determined using the classical Kurtz and Perry powder technique [17]. A Q switched Nd:YAG laser (QUANTA RAY Model LAB-170-10) beam of wavelength 1064 nm and a pulse width of 6 ns with a repetition rate of 10 Hz was used. The second harmonic generation was confirmed by the emission of green radiation of wavelength 532 nm. The second harmonic signal of 8.94 mJ and 22.1 mJ, respectively, were observed for KDP and GuCdS samples for an input signal of 0.70 J. Hence, the NLO test confirms that GuCdS has a SHG efficiency which is equal to 2.4 times that of KDP.

**Z-scan study:** Z-scan is the simplest and popular technique for the measurement of non linear refractive index and

nonlinear absorption coefficient of optical materials. It is an important technique which can be applied for the simultaneous measurement of magnitude and sign of nonlinear refractive index ( $n_2$ ) and nonlinear absorption coefficient ( $\beta$ ) of the material. The open aperture Z scan measurement is used to find the absolute value of nonlinear absorption coefficient ( $\beta$ ) and the closed aperture Z scan measurement is used to find the nonlinear refractive index ( $n_2$ ), using these values the real and imaginary part of nonlinear susceptibility ( $\chi_R^{(3)}$  and  $\chi_I^{(3)}$ ) can be calculated [18]. A continuous wave 50 mW diode pumped Nd:YAG laser of wavelength 632 nm was used in the experiment. The laser beam of radius 2 mm with the help of a convex lens of focal length 8.5 cm gives the intensity at the focus  $3.13 \text{ MW/cm}^2$ . The sample was moved along the optic axis (z direction) through the focus of the lens. The energy transmitted through an aperture was recorded as a function of sample position. The normalized transmission for the open aperture (OA) is shown in Fig. 8a. The transmission is minimum and symmetric with respect to the focus ( $Z=0$ ). This indicates that the sample exhibits reverse saturation absorption (RSA) with a positive nonlinear absorption coefficient, hence grown GuCdS crystal could be applied for optical limiting applications [18]. The normalized transmission for the closed aperture (CA) is shown in Fig. 8b. The peak to valley configuration of curve suggests that refractive index change is negative exhibiting a self-defocusing effect.

The calculated third order nonlinear optical parameters, such as nonlinear refractive index ( $n_2$ ), nonlinear absorption coefficient ( $\beta$ ), the real and imaginary part of nonlinear susceptibility ( $\chi_R^{(3)}$  and  $\chi_I^{(3)}$ ) are listed in Table-3.

Since, grown GuCdS crystal has a negative refractive index, it results in defocusing nature of the material which is an important as well as essential property for the application of material in optical sensors and night vision devices.

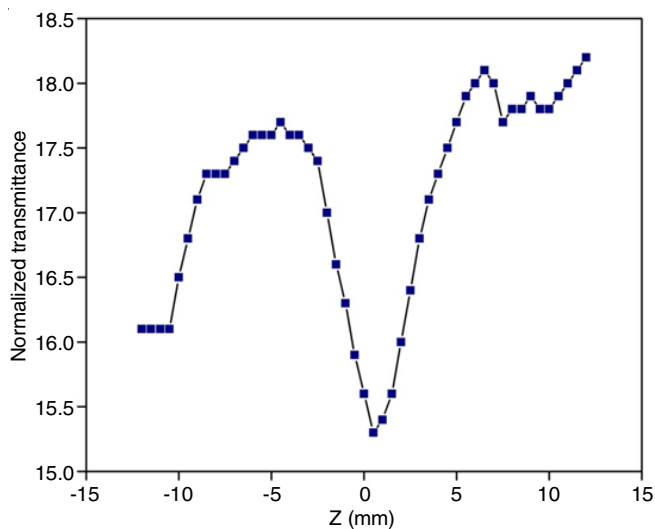


Fig. 8. (a) Open aperture curve of GuCdS

TABLE-3 NONLINEAR OPTICAL PARAMETERS OF GuCdS	
$n_2 \times 10^{-12} \text{ (cm}^2/\text{w)}$	-5.36
$\beta \times 10^{-4} \text{ (cm/w)}$	4.24
$\chi_R^{(3)} \times 10^{-10} \text{ (esu)}$	3.18
$\chi_I^{(3)} \times 10^{-7} \text{ (esu)}$	1.26
$\chi^{(3)} \times 10^{-4} \text{ (esu)}$	3.50

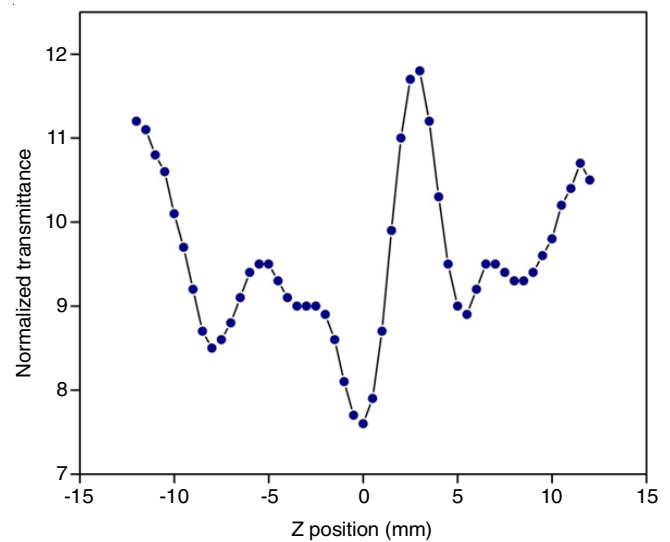


Fig. 8. (b) Closed aperture curve of GuCdS

**Dielectric study:** The dielectric studies of grown crystal were carried out at different frequencies. The single crystal of GuCdS with the dimension  $9.19 \text{ mm} \times 10.73 \text{ mm} \times 5.05 \text{ mm}$  was used for the dielectric measurement using HIOKI 3532 LCR HITESTER in the frequency range between 100 Hz and 5 MHz. The measurements were carried out in the range between the room temperature and  $105 \text{ }^\circ\text{C}$ . The crystal having silver coating on the opposite faces is placed between the two copper electrodes to form a parallel plate capacitor. The dielectric constant of crystal material was calculated using the following relation [19]:

$$\epsilon_r = \frac{Ct}{A\epsilon_0} \quad (7)$$

where C represents capacitance, A denotes the area of cross section,  $\epsilon_0$  is the permittivity of free space and t is the thickness of crystal. The variation of dielectric constant on frequency was studied at different temperatures is shown in Fig. 9.

From Fig. 9, it is notable that dielectric constant is high at lower frequency and starts decreasing gradually for higher frequencies. The dependence of dielectric constant with frequency

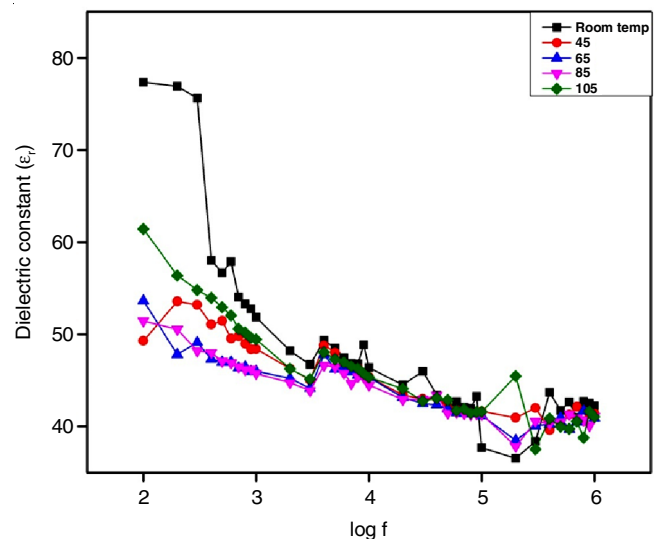


Fig. 9. Plot of dielectric constant with frequency of the applied electric field

shows almost similar behaviour for all temperatures. The electronic exchange of the number of ions in crystal gives local displacement of electron in the direction of applied field which in turn give rise to polarisation. The high value of dielectric constant in the low frequency region is attributed to contribution from all four polarizations namely: electronic, ionic, orientation and space charge polarizations. As the frequency of applied field increases and a point will be reached where the space charge cannot sustain and hence the dielectric constant starts to decrease. Hence, the gradual decline of dielectric constant at higher frequencies is attributed to the loss of significance of polarizations [20].

The variation of dielectric loss ( $\tan \delta$ ) with frequency of the applied field at different temperatures is shown in Fig. 10. Thus, it is clear that the dielectric loss values are high at lower frequencies and starts decreasing gradually for higher frequency. The low value of dielectric loss of grown crystal indicates that they are of good quality. Hence the gradual decreases of dielectric constant as well as the dielectric loss at higher frequency suggest that the crystal possesses enhanced optical quality with lesser defects which is an important parameter of nonlinear optical materials in their high speed electro-optic application.

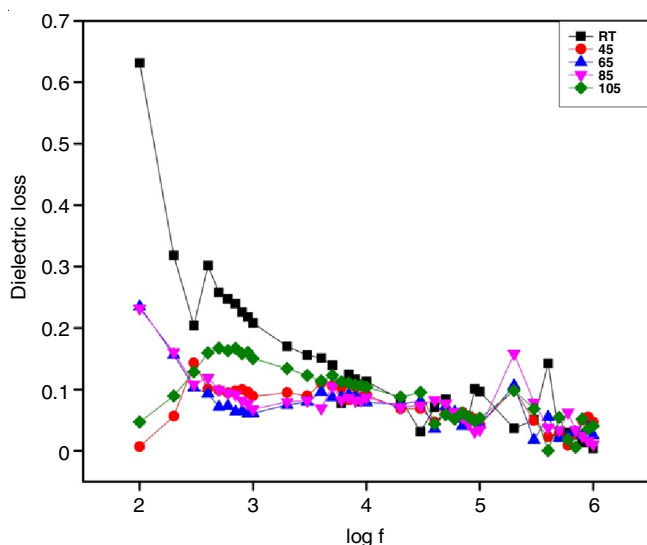


Fig. 10. Variation of dielectric loss with frequency of the applied electric field

**Laser damage threshold study:** The laser damage threshold study of nonlinear optical crystal is significant due to the fact that the surface damage threshold of crystal by high power laser limits its performance in nonlinear optical applications. In the present study, the laser damage threshold of grown GuCdS crystal was determined using a Q-switched high energy Nd:YAG laser of wavelength 1064 nm. The pulse width of 6 ns with a repetition rate of 10 Hz was used for this study. The laser beam was focussed on the crystal using a biconvex lens of focal length 15 cm. The surface damage threshold of grown crystal was calculated using the following relation [21]:

$$\text{Power density, } P_d = \frac{E}{\tau \pi r^2} \quad (8)$$

where  $E$  is the input energy (mJ),  $\tau$  represents the pulse width (ns) and  $r$  is the radius of spot (mm). The calculated value of

the laser damage threshold is 1.796 GW/cm<sup>2</sup> whereas for KDP it is 0.2 GW/cm<sup>2</sup>. Hence the high value of damage threshold indicates that the grown GuCdS crystal can be exploited for high power laser optical applications.

**Microhardness analysis:** Mechanical strength of material is an important parameter for device fabrication. In order to study the mechanical properties microhardness measurements were carried out on the smooth surface of the single crystal of GuCdS at room temperature using Futuretech FM 800 type E series hardness tester with diamond pyramidal indenter. Microhardness analysis was carried out for applied load ( $P$ ) varying from 1 g to 300 g. The Vickers microhardness number,  $H_v$  is calculated using the following relation [22]:

$$H_v = 1.854 \frac{P}{d^2} \text{ kg/mm}^2 \quad (9)$$

where  $P$  is the applied load in kg and  $d$  is the mean diagonal length of indentation in mm. A graph plotted between hardness number and the applied load is depicted in Fig. 11. The graph shows that the hardness values increases with the increase of load which is known as reverse indentation size effect.

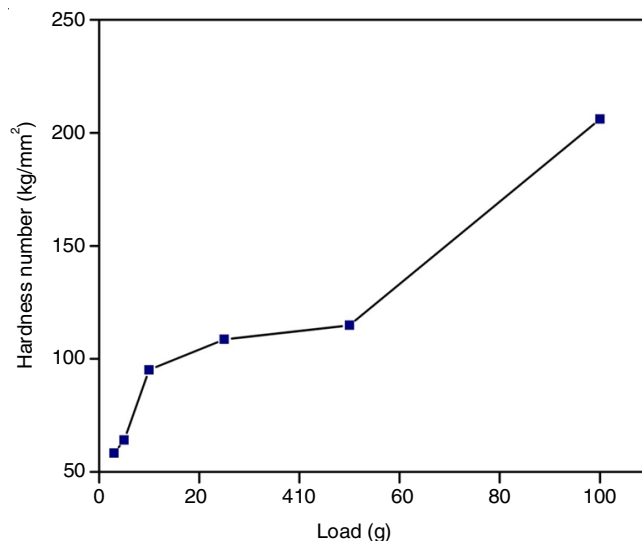


Fig. 11. Variation of microhardness number with applied load of GuCdS

Vickers hardness values of crystal increases with increase of load up to 100 g without any development of crack. For an indentation load of 300 g cracks were developed on the crystal surface around the indentation. This is due to the release of internal stress locally initiated by indentation. The maximum value of hardness number measured was 206.06 kg/mm<sup>2</sup> at the load of 100 g. The Vickers microhardness number,  $H_v$  of GuCdS crystal is compared with that of guanidine derivative compounds such as guanidinium trifluoroacetate, guanidinium perchlorate, guanidinium manganese sulphate and the results are presented in Table-4. The superior hardness value of grown GuCdS crystal indicates that the greater stress is required to form dislocations, thus ensuring greater crystalline perfection.

The work hardening coefficient ( $n$ ) was calculated from Mayer's relation ( $P$ ) =  $Kd^n$  connecting load  $P$  and average diagonal length  $d$  of indentation,  $K$  is the material constant. The work hardening coefficient ( $n$ ) of grown crystal was determined from the plot of  $\log P$  against  $\log d$  for GuCdS crystal and is shown

TABLE-4  
COMPARISON OF VICKERS HARDNESS VALUE OF GuCdS  
WITH OTHER GUANIDINIUM BASED CRYSTALS

Compound	Vickers microhardness (kg/mm <sup>2</sup> )	Ref.
Guanidinium manganese sulphate	78.56 at 50 g	[23]
Guanidinium trifluoroacetate	59.00 at 60 g	[24]
Guanidinium perchlorate	60.50 at 40 g	[25]
Guanidinium cadmium sulphate	206.06 at 100 g	Present study

in Fig. 12. From the linear fit of plot, the slope of straight line yields the value of  $n$  as 2.26.

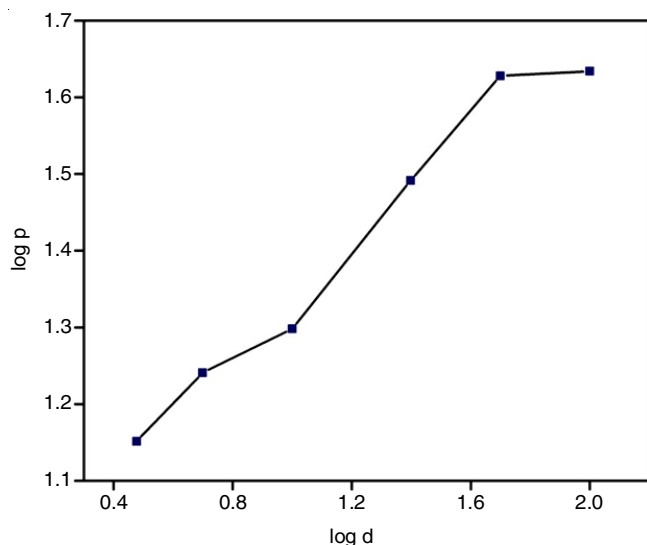


Fig. 12. Variation of diagonal length of indentation with load

According to Onitsch,  $n$  should lie between 1 and 1.6 for hard material and is more than 1.6 for soft material. Hence the value of  $n$  indicates that GuCdS crystal belongs to soft material category. The yield strength of crystal ( $\sigma_y$ ) and elastic stiffness constant ( $C_{11}$ ) were calculated using the following expressions [23]:

$$\sigma_y = \frac{H_v}{3} (0.1)^{(n-2)} \quad (10)$$

$$C_{11} = H_v^{7/4} \quad (11)$$

The obtained values of yield strength and stiffness constant for different loads are listed in Table-5. Elastic stiffness constant  $C_{11}$  gives the idea of tightness of bonding between the neighbouring atoms and was found to be in the range of 573-394363 GPa. Yield strength of the crystal was found to be in the range of 10.68-37.74 MPa. Hence, the hardness study of grown GuCdS

TABLE-5  
MECHANICAL PROPERTIES OF GuCdS CRYSTAL

Load P (g)	Hardness number $H_v$ (kg/mm <sup>2</sup> )	Yield strength $\sigma_y$ (MPa)	Elastic stiffness constant $C_{11}$ (GPa)
3	58.37	10.68	573
5	64.13	11.74	1111
10	72.56	17.42	17626
25	108.69	19.90	44654
50	114.87	21.03	65895
100	206.06	37.74	394363

crystal revealed that it has sufficient mechanical strength for non-linear optical device fabrication.

**Thermal studies:** Thermal stability of GuCdS was examined by thermogravimetric (TG) and differential thermogravimetric analyses (DTG) in order to study the phase transition, melting point and various stages of decomposition. Using TG-DTG curve, the decomposition temperature and the percentage mass loss at each stage can be easily determined. The GuCdS sample initially weighing 13.035 mg was heated in an alumina crucible in nitrogen atmosphere at the flow rate of 20 mL/min. The crystalline sample was heated in the temperature range between 25 and 1400 °C and the thermogram is shown in Fig. 13. A careful examination of TG curve elucidates the occurrence of four stage weight loss pattern and it is also evident that GuCdS compound is stable upto 105 °C. The first stage weight loss occurred between 105 °C and 122 °C eliminating 11.71 % of the initial mass which is due to the evaporation of water molecule in the sample. The DTG curve shows the corresponding sharp peak at the same temperature range. The second stage weight loss was observed between 122 °C and 174 °C with a weight loss of about 7.3 % due to the decomposition of guanidinium compound with the release of ammonia. The third and fourth stage of decomposition experience the major weight losses of about 30.97 % and 49.33 % between the temperatures 907 and 1250 °C. The decomposition process was carried out upto 1400 °C and the residual mass was stabilized at 0.39 % of the initial mass. The sharp DTG peaks appeared in the thermogram indicates the good crystalline nature of grown crystal. From the thermal analysis, it is clear that GuCdS crystal can be employed for practical applications upto 105 °C.

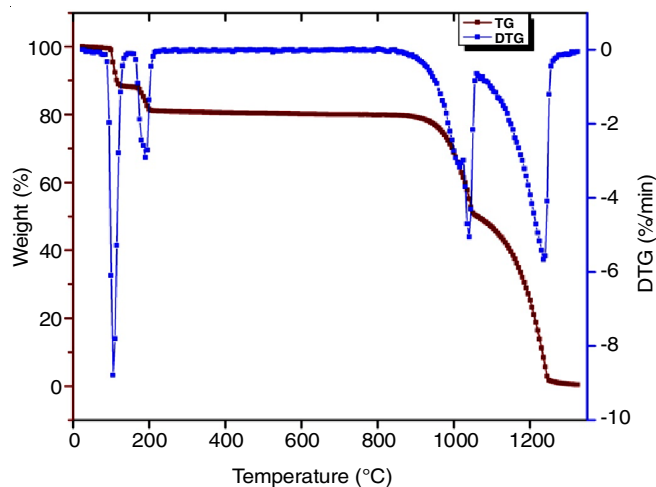


Fig. 13. TG-DTG curve of GuCdS crystalline sample

## Conclusion

A potential semi-organic nonlinear optical single crystal of guanidinium tris cadmium sulphate octahydrate (GuCdS) was grown from its aqueous solution by slow evaporation technique. Powder X-ray diffraction analysis confirmed that the grown crystal belongs to triclinic system with space group  $P\bar{1}$ . The FTIR analysis revealed the functional groups present in GuCdS compound and their different modes of vibrations. The UV-vis-NIR spectral studies elucidated that GuCdS crystal has 80 % transmission in the entire visible and NIR region thus

confirming the suitability of grown crystal for optical applications. The band gap value was found to be 6.14 eV. The refractive index, extinction coefficient and optical conductivity were calculated using the optical transmission data. The second harmonic generation efficiency was calculated to be 2.4 times that of KDP. The third order nonlinear optical parameters such as nonlinear refractive index, nonlinear absorption coefficient and the real and imaginary part of nonlinear susceptibilities were calculated using Z-scan technique. The variation of dielectric constant with applied field frequency and temperature were analyzed and it was found that the crystal exhibits low dielectric loss which is an important property for NLO application. From microhardness study, it was found that the crystal belongs to soft material category. The crystal exhibits high laser damage threshold value of 1.796 GW/cm<sup>2</sup> which is a favourable property for nonlinear applications. The Vicker's microhardness values measured indicates the high mechanical strength of the crystal. From TG-DTG curves, it is evident that the material is stable up to 105 °C. Thus optical, mechanical and electrical properties of grown GuCdS crystal indicate the suitability of crystal for future photonic applications.

#### ACKNOWLEDGEMENTS

One of the authors (AR) is grateful to SAIF, IIT-M for the characterisation techniques and also to the Management of Loyola College, Chennai, India for providing hardness study.

#### CONFLICT OF INTEREST

The authors declare that there is no conflict of interests regarding the publication of this article.

#### REFERENCES

1. S. Arjunan, A. Bhaskaran, R.M. Kumar and R. Jayavel, *J. Alloy Compd.*, **506**, 784 (2010); <https://doi.org/10.1016/j.jallcom.2010.07.070>.
2. W. Wang, K. Sutter, C.P.Z. Bosshard, H. Arend, P. Gunter, G. Chapius and F. Nicolo, *Jpn. J. Appl. Phys.*, **27**, 1138 (1998); <https://doi.org/10.1143/jjap.27.1138>.
3. N. Zhang, M. Jiang, D. Yuwan, D. Xu and X. Tao, *Chin. Phys. Lett.*, **6**, 280 (1989); <https://doi.org/10.1088/0256-307x/6/6/011>.
4. R.J. Sension, B. Hudson and P.R. Callis, *J. Phys. Chem.*, **94**, 4015 (1990); <https://doi.org/10.1021/j100373a026>.
5. O.D. Bonner and C.F. Jordon, *Spectrochim Acta Part A Mol. Spectrosc.*, **32**, 1243 (1976); [https://doi.org/10.1016/0584-8539\(76\)80316-9](https://doi.org/10.1016/0584-8539(76)80316-9).
6. M. Fleck, L. Bohaty and E. Tilmanns, *Solid State Sci.*, **6**, 469 (2004); <https://doi.org/10.1016/j.solidstatesciences.2004.02.008>.
7. M.J. Bushri, C.J. Antony and M. Fleck, *Solid State Commun.*, **143**, 348 (2007); <https://doi.org/10.1016/j.ssc.2007.05.024>.
8. P.M. Nikolic, *J. Phys. Condens. Matter.*, **5**, 3039 (1993); <https://doi.org/10.1088/0953-8984/5/18/026>.
9. T. Arumanayagam and P. Murugakoothan, *Mater. Lett.*, **65**, 2748 (2011); <https://doi.org/10.1016/j.matlet.2011.05.081>.
10. A. Suvitha, V. Satyanarayanamoothy and P. Murugakoothan, *Spectrochim. Acta Part A Mol. Biomol. Spectrosc.*, **110**, 255 (2013); <https://doi.org/10.1016/j.saa.2013.02.025>.
11. M.J. Bushri and C.J. Antony, *J. Raman Spectrosc.*, **39**, 368 (2008); <https://doi.org/10.1002/jrs.1828>.
12. G. Shanmugam and S. Brahadeeswaran, *Spectrochim. Acta Part A Mol. Biomol. Spectrosc.*, **95**, 177 (2012); <https://doi.org/10.1016/j.saa.2012.04.100>.
13. S. Natarajan, G. Shanmugam and S.A.M. Britto Dhas, *Cryst. Res. Technol.*, **43**, 561 (2008); <https://doi.org/10.1002/crat.200711048>.
14. R.M. Jauhar, S. Kalainathan and P. Murugakoothan, *J. Cryst. Growth*, **424**, 42 (2015); <https://doi.org/10.1016/j.jcrysgro.2015.05.003>.
15. R. Subhasini, D. Sathya, V. Sivashankar, P.S. Latha Mageshwari and S. Arjunan, *Opt. Mater.*, **62**, 357 (2016); <https://doi.org/10.1016/j.optmat.2016.09.041>.
16. T. Arumanayagam and P. Murugakoothan, *J. Miner. Mater. Charact. Eng.*, **10**, 13 1225 (2011); <https://doi.org/10.4236/jmmce.2011.1013095>.
17. S.K. Kurtz and T.T. Perry, *J. Appl. Phys.*, **39**, 3798 (1968); <https://doi.org/10.1063/1.1656857>.
18. K. Senthil, S. Kalainathan, A. Ruban Kumar and P.G. Aravindan, *RSC Adv.*, **4**, 56112 (2014); <https://doi.org/10.1039/c4ra09112d>.
19. A. Cyrac Peter, M. Vimalan, P. Sagayaraj and J. Madhavan, *Phys. B: Cond. Matter.*, **405**, 65 (2010); <https://doi.org/10.1016/j.physb.2009.08.035>.
20. F.M. Reicha, M. El-Hiti, A.Z. El-Sonabati and M.A. Diab, *J. Phys. D: Appl. Phys.*, **24**, 369 (1991); <https://doi.org/10.1088/0022-3727/24/3/020>.
21. S. Manivannan, S. Dhanuskodi, S.K. Tiwari and J. Philip, *Appl. Phys. B*, **90**, 489 (2008); <https://doi.org/10.1007/s00340-007-2911-4>.
22. B. Lal, K.K. Bamzai, P.N. Kortu and B.M. Wanklyn, *Mater. Chem. Phys.*, **85**, 353 (2004); <https://doi.org/10.1016/j.matchemphys.2004.01.013>.
23. A. Rajeswari, G. Viniitha and P. Murugakoothan, *J. Mater. Sci.: Mater. Electr.*, **29**, 12526 (2018); <https://doi.org/10.1007/s10854-018-9352-1>.
24. M. Loganayaki, V.S. Sankar, P. Ramesh, M.N. Ponnuswamy and P. Murugakoothan, *J. Mater. Mater. Charact. Eng.*, **10**, 843 (2011); <https://doi.org/10.4236/jmmce.2011.109065>.
25. V. Sivashankar, R. Siddheswaran and P. Murugakoothan, *Mater. Chem Phys.*, **130**, 323 (2011); <https://doi.org/10.1016/j.matchemphys.2011.06.053>.